JACS
JOURNAL OF THE AMERICAN CHEMICAL SOCIETY
Article
Cite This: J. Am. Chem. Soc. 2019, 141, 14239−14248
pubs.acs.org/JACS

Folding and Assembly of Short α, β, γ-Hybrid Peptides: Minor Variations in Sequence and Drastic Differences in Higher-Level Structures

Yukun Zhang,[†,§,⊗] Yulong Zhong,[‡,⊗] Alan L. Connor,[‡] Daniel P. Miller,[‡] Ruikai Cao,[‡] Jie Shen,[∥] Bo Song,[⊥] Erin S. Baker,[#] Quan Tang,[¶] Surya V. S. R. K. Pulavarti,[‡] Rui Liu,[¶] Qiwei Wang,[†] Zhong-lin Lu,[¶] Thomas Szyperski,[‡] Huaqiang Zeng,[∥] Xiaopeng Li,[⊥] Richard D. Smith,[#] Eva Zurek,[‡] Jin Zhu,[*,†] and Bing Gong[*,‡]

[†]Chengdu Institute of Organic Chemistry, Chinese Academy of Sciences, Chengdu 610041, China
[‡]Department of Chemistry, University at Buffalo, The State University of New York, Buffalo, New York 14260, United States
[§]University of Chinese Academy of Sciences, Beijing 100049, China
[∥]The NanoBio Lab, 31 Biopolis Way, The Nanos 138669, Singapore
[⊥]Department of Chemistry, University of South Florida, Tampa, Florida 33620, United States
[#]Biological Sciences Division, Pacific Northwest National Laboratory, Richland, Washington 99354, United States
[¶]College of Chemistry, Beijing Normal University, Beijing 100875, China

Supporting Information

ABSTRACT: Multilevel protein structures typically involve polypeptides of sufficient lengths. Here we report the folding and assembly of seven short tetrapeptides sharing the same types of α-, β-, and aromatic γ-amino acid residues. These are two sets of hybrid peptides, with three members in one set and four in the other, having complementary hydrogen-bonding sequences that were hypothesized to pair into linear H-bonded duplexes. However, instead of undergoing the anticipated pairing, the initially examined three oligomers, **1** and **2a** or **2b**, differing only in their central αβ hybrid dipeptide sequence, do not associate with each other and exhibit distinctly different folding behavior. Experiments based on NMR and mass spectrometry, along with computational studies and systematic inference, reveal that oligomer **1** folds into an expanded β-turn containing an unusual hybrid α/β-amino acid sequence composed of glycine and β-alanine, two α- and β-amino acid residues that are conformationally most flexible, and peptides **2a** and **2b** adopt a noncanonical, extended helical conformation and dimerize into double helices undergoing rapid conformational exchange or helix inversion. The different central dipeptide sequences, αβ vs βα, result in drastically different intramolecular H-bonding patterns that are responsible for the observed folding behavior of **1** and **2**. The revealed turn and double helix have few natural or synthetic counterparts, and provide novel and unique folding prototypes based on which chiral α- and β-amino acids are incorporated. The resultant derivatives **1a**, **1b**, **2c**, and **2d** follow the same folding and assembling behavior and demonstrate the generality of this system with the formation of expanded β-turns and double helices with enhanced folding stabilities, hampered helix inversion, as well as defined and dominant helical sense. This work has demonstrated the unique capability of synthetic foldamers in generating structures with fascinating folding and assembling behavior. The revealed systems offer ample opportunity for further structural optimization and applications.

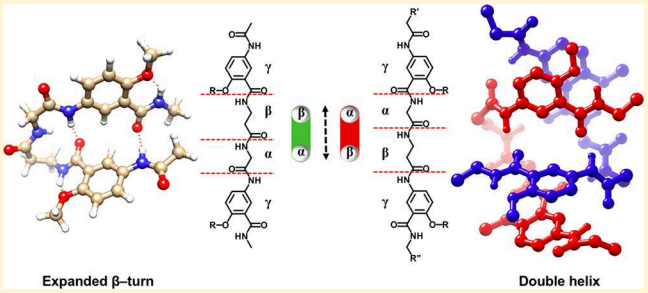

INTRODUCTION

The folding of biomacromolecules has inspired the development of foldamers,[1] i.e., oligomers having abiotic backbones with defined conformations, for mimicking biological folding or uncovering folding and other behavior not seen in nature. The majority of known foldamers adopt helical conformations reminiscent of the α-helix and other single-stranded helices, with representative systems including peptidomimetic foldamers such as β-,[2,3] γ-,[4] and δ-peptides,[5] aliphatic oligoureas,[6] and peptoids;[7] and abiotic foldamers such as oligo(phenylene ethynylenes),[8] aromatic oligoamides,[9] hydrazides,[10] and oligoureas,[11] as well as other foldamers consisting of aromatic residues.[12] In contrast, nonhelical foldamers, like those adopting turns,[13] sheets,[14,15] or other conformations,[16] are still rare. Compared to biological foldamers, synthetic

Received: June 7, 2019
Published: August 5, 2019

DOI: 10.1021/jacs.9b06094
J. Am. Chem. Soc. 2019, 141, 14239−14248

foldamers can accommodate a much wider range of building blocks and covalent linkages,[17] and offer designs that are limited only by one's imagination. Consequently, oligomeric molecules with a great variety of primary structures can be made available on the basis of the basic principles of physical organic and synthetic chemistry, which allows distinct folding behavior and folded structures that mimic or differ from those of biomacromolecules to be uncovered.

Herein we report the folding and assembly of oligomers **1** and **2**, hybrid tetrapeptides having α-, β-, and aromatic γ-amino acid residues and differing only in their central $\alpha\beta$ dipeptide segments (Figure 1). In spite of their short length, these hybrid peptides exhibit distinctly different folding and assembling behavior, as shown by their lack of mutual association, their H-bonded amide protons, and their dissimilar ^{1}H NMR spectra, which, though initially perplexing, could eventually be understood based on an interactive feedback loop between experimental analysis, computational studies, and systematic inference. Two novel secondary structures, one being an unusual hairpin or an expanded β-turn with a loop consisting of an α- and a β-amino acid residue, and the other an extended helix that associates into interconverting double helices, have been identified. The folding and assembly of these hybrid peptides, which involve multistructural levels typically associated with proteins, are surprisingly sophisticated and found with few other synthetic foldamers.

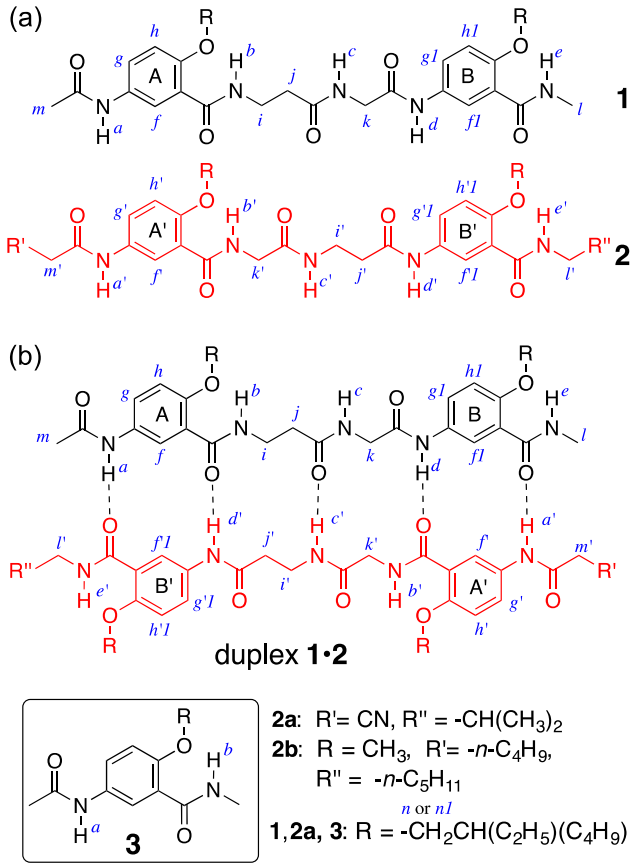

Figure 1. (a) Structures of hybrid peptides **1** and **2**. (b) The expected H-bonded duplex **1·2**. Labels of most hydrogens and the two aromatic residues are shown. Compound **3** corresponds to the aromatic residues of **1** and **2**.

We previously developed H-bonded duplexes composed of linear oligoamide strands carrying arrays of H-bond donors and acceptors.[18] With their programmable sequence-specificity, our H-bonded duplexes served as molecular association units for forming templated β-sheets,[19] supramolecular block copolymers,[20] and for the specification of chemical reactions.[21] While hetero- and homoduplexes with even numbers of H-bonds have been well characterized,[18] duplexes having odd numbers of interstrand H-bonds, which will only allow heteroduplexes to form, have not been made.

Tetrapeptides **1** and **2a**/**b** (Figure 1a) differ in the sequences of their central α/β-dipeptide segments, i.e., βAla-Gly of **1** and Gly-βAla of **2**, that are flanked by the same aromatic γ-amino acid residues at their C- and N-termini. The racemic 2-ethylhexyl group, widely used in solubilizing various oligomers and polymers,[22] was initially chosen and incorporated into **1** and **2a**. Four other oligomers, **1a**/**b** and **2c**/**d**, derived from **1** and **2a**/**b** are also designed and studied (see Figure 8). Apparently, other side (R) chains and end (R′ and R′′) groups can also be incorporated. If adopting extended conformations, oligomers **1** and **2** should pair into duplex **1·2** by forming five intermolecular H-bonds (Figure 1b) involving amide protons *a* and *d* of **1**, and *a*′, *c*′, and *d*′ of **2**. Protons *b* and *e* of **1**, and protons *b*′ and *e*′ of **2**, being parts of highly favorable six-membered H-bonded rings, should remain intramolecularly H-bonded under most conditions as demonstrated by numerous previous, including our own, studies.[18b,23]

RESULTS AND DISCUSSION

Observations on the Surprising Lack of Interaction between 1 and 2, Dissimilar ^{1}H NMR Spectra, and Conformational Exchange. The anticipated association of **1** and **2** was first examined by comparing the chemical shifts of protons *a* and *d* of **1**, and *a*′, *c*′, and *d*′ of **2**, to those of the same protons in the 1:1 mixture of the two oligomers. Forming the H-bonded duplex **1·2** should result in large (1 to 2 ppm) downfield shifts of these amide protons.[28] Surprisingly, compared to the amide ^{1}H resonances of single strands **1** and **2a**, these protons exhibited small, mostly negligible changes in their chemical shifts upon mixing the two oligomers (1:1) at 1, 10, and 50 mM (Table S1). The insignificant shifts in the resonances of these five protons indicate very weak, if any, H-bonding interaction between the two oligomers.

Compared to proton *a* of **3** (1 mM in $CDCl_3$) that appears at 7.22 ppm and undergoes negligible H-bonding at this concentration,[18b] the signals of protons *a* and *d* of **1**, and *a*′ and *d*′ of **2a** (or **2b**), also at 1 mM in $CDCl_3$, show very large (1.8 to 2.8 ppm) downfield shifts, indicating that, although **1** and **2** do not associate with each other, their amide protons do engage in H-bonding with H-bond donors of their own molecules.

In addition to the apparent lack of H-bonding interactions between **1** and **2a**, the ^{1}H NMR spectra of the two peptides bear no similarity (Figure 2). The spectrum of **1** contains sharp, well-dispersed signals indicating the presence of a well-defined species (Figure 2a). The fact that the amide and aromatic ^{1}H NMR signals of **1** can be completely assigned to the backbone protons suggest that the two racemic 2-ethylhexyl side chains do not result in observable diastereotopic signals for the backbone protons of **1**.

By contrast, the spectrum of **2a** contains both sharp and broadened peaks (Figure 2b), including the severely broadened signals of protons *i*′ and *k*′, the broadened

DOI: 10.1021/jacs.9b06094
J. Am. Chem. Soc. 2019, 141, 14239−14248

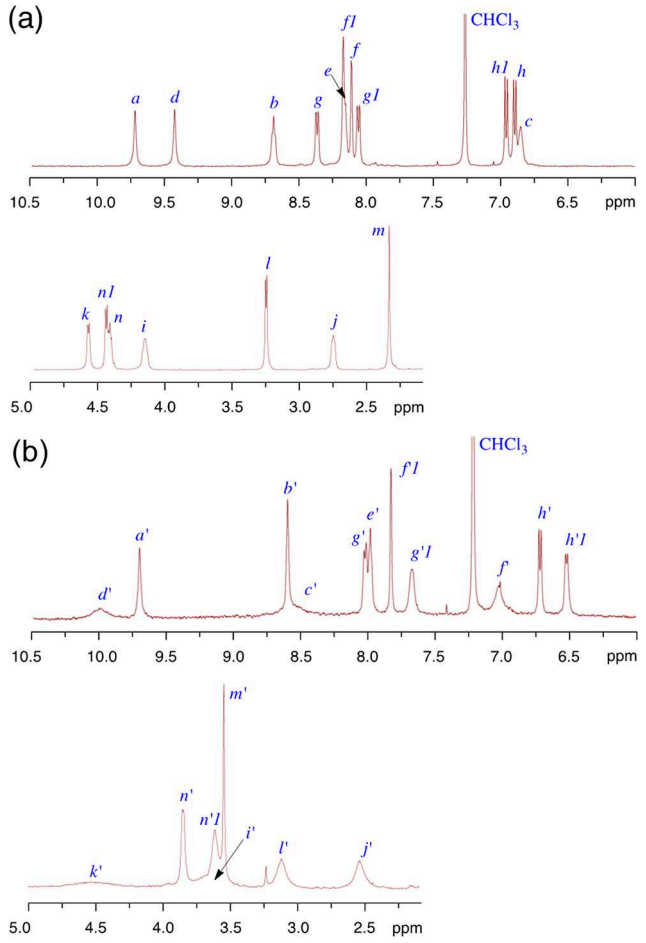

Figure 2. 500 MHz partial ^{1}H spectra of (a) **1** (5 mM) and (b) **2a** (5 mM) at 25 °C in $CDCl_3$.

resonances of protons *c*′ and *d*′, and the moderately broadened peaks of protons *f*′, *j*′, and *l*′. The resonances of the other amide and aromatic protons of **2a** remain sharp. The presence of both sharp and broad peaks in the spectrum of **2a** rules out the formation of poorly defined higher aggregates. Instead, the line-broadening observed with only some of the proton resonances of **2a** is typical of chemical exchange caused by conformational interconversion in the microsecond to millisecond time scale.[24]

Oligomer **2b**, which shares the same amino acid sequence with **2a** but has methyl side chains and linear end groups, gives a ^{1}H NMR spectrum that only differs from that of **2a** in the chemical shifts of protons *a*′ and *m*′ (Figures S1) due to the electron-withdrawing cyano group of **2a**. Like those of **2a**, the peaks of protons *i*′ and *k*′ of **2b** are severely broadened; and the signals of *c*′, *d*′, and *j*′ are broadened. The same conformational interconversion observed with both **2a** and **2b**, which differ in their side chains and end groups, can only be attributed to the same tetrapeptide backbone shared by the two oligomers. The very similar ^{1}H NMR spectra of **2a** and **2b** also suggest that their different side chains have no influence on the resonances of their backbone protons.

The H-bonded amide protons that do not lead to the association of **1** and **2**, along with the different ^{1}H NMR spectra of the two otherwise similar hybrid peptides, suggest that H-bonds involving the amide protons of **1** or **2** mainly act by either stabilizing folded conformation(s) or facilitating the self-association of each peptide.

Distinct H-Bonding Behavior and the Dimerization of 2. To understand the unexpected and puzzling lack of association between **1** and **2**, inter- and intramolecular H-bonding interactions involving the amide protons of these oligomers were systematically examined against concentration, temperature, and solvent polarity.

The Influence of Concentration. Among the amide hydrogens of **1**, only proton *c* shows a significant (0.66 ppm) downfield shift from 0.1 to 25 mM in $CDCl_3$ (Table S2a), indicating that this proton becomes increasingly involved in intermolecular H-bonding with rising concentration. Similar to the signals of protons *b* and *e* that are intramolecularly H-bonded, the resonances of protons *a* and *d* also exhibit very small shifts in this concentration range, suggesting that these protons are intramolecularly H-bonded. Given its sharp ^{1}H resonances, peptide **1** seems to exist as a single species. From 3 to 25 mM in $CDCl_3$, amide protons *c*′ and *d*′ of **2a** shift downfield by 0.16 and 0.13 ppm, respectively and proton *a*′ shows an insignificant shift (Table S2b). The concentration-dependent shifts observed with protons *c*′ and *d*′ imply that **2a** self-associates via intermolecular H-bonding interactions.

The Role of Temperature. From 0 to 45 °C in $CDCl_3$, the signals of protons *a* and *d* of **1** (5 mM) shift upfield by 0.33 and 0.22 ppm, respectively (Table S3a), suggesting that the intramolecular H-bonds involving protons *a* and *d* are sensitive to rising temperature. The small upfield shift (~0.06 ppm) of proton *c* indicates that H-bonding involving proton *c* is negligible at 5 mM. From 0 to 45 °C, the resonances of protons *c*′ and *d*′ of **2a** (5 mM in $CDCl_3$) exhibit noticeable upfield shifts of 0.42 and 0.41 ppm, respectively, which points to weakened H-bonding and indicates that protons *c*′ and *d*′ are intermolecularly H-bonded (Table S3b). Proton *a*′ shows a small (<0.1 ppm) shift, implying that it may either be intramolecularly H-bonded or not H-bonded.

At −45 °C, all of the ^{1}H resonances of **2a** and **2b** turn sharp (Figures S2), which confirms that the broadened ^{1}H resonances of **2a** and **2b** at room temperature are due to conformational interconversion that slows down with decreasing temperature. At −45 °C, the protons of each of the Gly and *β*Ala methylene groups, i.e., protons *i*′, *j*′, or *k*′, appear as two well separated peaks, indicating that bond rotation involving these methylene carbons is restricted due to slowed conformational interconversion, resulting in nonequivalent protons.

The Effect of Solvent Polarity. The H-bonding interactions of **1** and **2** were further studied in $CDCl_3$ containing DMSO-d_6. Among the amide protons of **1**, proton *c* shows a downfield shift of ~1 ppm as the ratios of DMSO-d_6 increased from 0 to 15% (Figure 3a and Table S4a), confirming that proton *c* is exposed to solvent molecules. In comparison, the resonances of the other amide protons exhibit much smaller shifts, indicating that **1** adopts a conformation in which these protons are shielded from solvent molecules and are intramolecularly H-bonded. The amide protons of **2a** responded very differently to changing solvent polarity (Figure 3b and Table S4b). At 5 mM with 0 to 15% DMSO-d_6, the signals of protons *c*′ and *d*′ undergo 1.04 and 0.58 ppm, respectively, *upfield* shifts, indicating that the intermolecular H-bonds between the molecules of **2a** are weakened or interrupted by DMSO molecules. In contrast, the signal of proton *a*′ shows a noticeable (0.30 ppm) downfield shift, indicating that proton *a*′ of **2a** is exposed to solvent molecules.

DOI: 10.1021/jacs.9b06094
J. Am. Chem. Soc. 2019, 141, 14239−14248

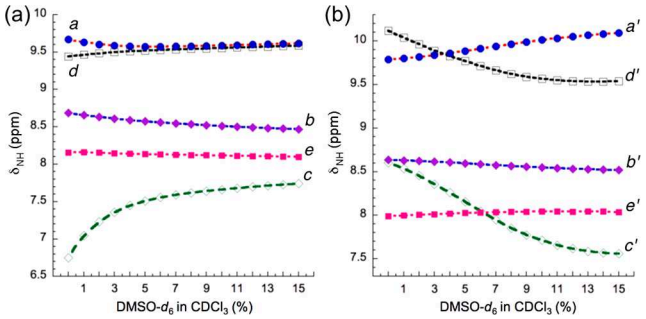

Figure 3. Chemical shift δ_{NH} of amide protons of (a) **1** (5 mM) and (b) **2a** (5 mM) versus percent of DMSO-d_6 in $CDCl_3$.

Evidence from ^{1}H NMR studies thus indicates that, except for proton *c*, the other amide protons of **1** are intramolecularly H-bonded. Proton *a*′, which shows no shift with changing concentration or temperature but moves downfield with increasing proportion of DMSO, seems to be exposed to solvent molecules and does not participate in the self-association of **2a**. Protons *c*′ and *d*′, with their resonances shifting noticeably with changing concentration, temperature, and ratio of polar solvent, must be involved in intermolecular H-bonding that facilitates the self-association of **2a**.

Dimerization of **2**. Protons *c*′ and *d*′ of **2b** show concentration-dependent shifts (Figure S3) that fit satisfactorily into a dimerization model,[18b] giving a dimerization constant of 7×10^3 M^{-1}, a value close to those of linear 4-H-bonded duplexes we reported before,[18b] implying that tetrapeptides **2** may be undergoing dimerization via four intermolecular H-bonds.

That oligomer **2** indeed undergoes dimerization was confirmed by examining **2b** with electrospray ionization-mass spectrometry (ESI-MS) and traveling wave ion mobility-mass spectrometry (TWIM-MS). In $CHCl_3$ with different ratios of CH_3OH (Figure S4a), the dimers of **2b** exist as the major species in the least polar solvent ($CHCl_3/CH_3OH$ = 9/1); in $CHCl_3/CH_3OH$ (1/1), the dimers and monomers of **2b** exist in similar abundance; in $CHCl_3/CH_3OH$ (1/9), oligomer **2b** exists mainly as its monomers. These results are fully consistent with the H-bonded nature of **2b** dimer. In addition, tandem mass spectrometry indicated that the dimers of **2b** fully associate into the monomers at 22 V (Figure S4b).

The effects of concentration, temperature, and solvent polarity on the resonances of amide protons suggest that tetrapeptide **1** folds into a monomeric conformation that is stabilized by H-bonds involving protons *a* and *d*, while proton *c* does not engage in intramolecular H-bonding. Peptide **2**, with its protons *c*′ and *d*′ engaging in intermolecular H-bonding, exists as dimers as confirmed by mass spectrometry. Besides, peptide **2** undergoes conformational interconversion that slows down at low temperature.

Likely Conformations and Assembly of 1 and 2. On the basis of the results and conclusions from NMR and mass spectral studies, the likely conformations of **1** and **2** are deduced. As shown in Figure 4a, to exist as monomers with protons *a* and *d*, but not *c*, being intramolecularly H-bonded, the only reasonable conformation of peptide **1** is hairpin **1A** in which the two aromatic residues are H-bonded. Hairpin **1A** is an unusual, expanded β-hairpin with a loop consisting of an α-amino acid (glycine) residue and a β-amino acid (β-alanine) residue.

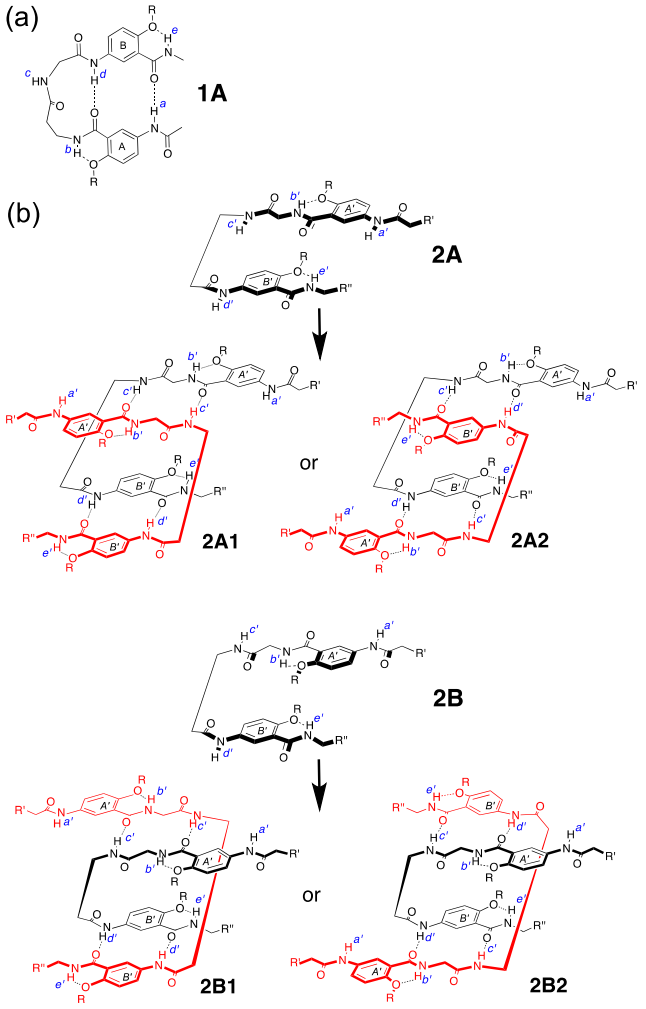

Figure 4. Illustration of the possible conformations of (a) **1** and (b) **2** deduced from data based on 1D ^{1}H NMR and mass spectral studies. H-bonds are shown as dashed lines. Some of the bonds are not drawn in proportion for clarity.

The likely conformations of **2** are presented in Figure 4b. Protons *c*′ and *d*′, along with the two benzamide oxygen atoms of **2**, constitute an array of four H-bond donors and acceptors. To dimerize, peptide **2** has to adopt a bent conformation, which is only possible if the ethylene linker of the βAla residue dissects the array of the four H-bond donors and acceptors into two segments, one involving the Gly residue flanked by proton *c*′ and a benzamide oxygen, and the other being the aromatic residue B′ flanked by proton *d*′ and the other benzamide oxygen. Two different bent conformations, **2A** and **2B**, are possible. In **2A**, N−H*c*′ and N−H*d*′ bonds, and the two benzamide C═O bonds point to the same side; in **2B**, N−H*c*′ and N−H*d*′ bonds, along with their adjacent C═O bonds, point to different directions.

Two different dimers, **2A1** and **2A2**, or **2B1** and **2B2**, could be formed based on **2A** or **2B**, depending on whether the same or different segments of the two molecules are H-bonded together. Each dimer of **2A** has its four intermolecular H-bonds arranged roughly in a plane that separate the two constituent molecules, while the dimers based on **2B** have their two constituent molecules wrapping around each other, forming double helices.

DOI: 10.1021/jacs.9b06094
J. Am. Chem. Soc. 2019, 141, 14239−14248

Revelation of the Conformations and Assembly of 1 and 2 Based on Computational Studies. Monomer **1A** and the four possible dimers of **2** were optimized with dispersion-corrected density functional theory (DFT) computations[25] carried out with the ADF software package.[26] Further computational details can be found in the Supporting Information. Conformation **1A** was optimized to a hairpin structure, i.e., a novel expanded β-turn[28] involving an 11-atom, intramolecularly hydrogen-bonded ring with a hybrid α/β amino acid sequence consisting of Gly and βAla residues (Figure 5a). The O···H distances in the two intramolecular H-bonds involving protons *a* and *d* are 1.93 and 1.99 Å, respectively, while proton *c* does not engage in intramolecular H-bonding.

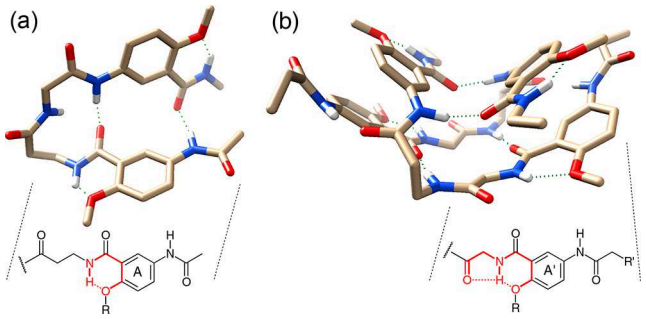

Figure 5. (a) Energy-minimized structures of **1A** and (b) dimer **2B1**. The side chains of **1** and **2** and the end groups R′ and R″ of **2** are replaced with methyl groups. Hydrogen bonds are indicated as dashed dark green lines. All H atoms, except for those of amide groups, are removed for clarity. The intramolecular H-bonded rings involving the βAla or Gly residue and aromatic residue A or A′ are shown under each optimized structure.

The computationally optimized structures and relative energies of dimers **2A1**, **2A2**, **2B1**, and **2B2** (Figure S5) indicate that **2B1** and **2B2** are much more stable ($\Delta\delta E$ > 16−21 kcal/mol, see Table S5) than either **2A1** or **2A2**. Comparing the optimized structures of the four dimers indicate that in **2A1** or **2A2**, oligomer **2** adopts a strained, bent conformation, and the aromatic rings and amide linkages are not positioned to allow the existence of any stacking interactions, while in **2B1** or **2B2**, oligomer **2** adopts a relaxed, extended helical conformation that engages in stacking interactions involving the aromatic rings and amide groups. The energetic and structural differences revealed by computational studies thus suggest that **2** most likely exists as conformation **2B1** and **2B2**, two extended helices.

Between the two possible dimers of **2B**, dimer **2B1** is 4.5 kcal/mol more stable than **2B2**. Comparing the optimized structures of **2B1** and **2B2** indicates that in dimer **2B1** (Figure 5b), the two pairs of benzene rings are placed within stacking distance of each other (C−C distances of ∼3.3−4.1 Å, cf. 3.9−4.1 Å calculated for the benzene dimer), while in **2B2** (Figure S5), only one pair of benzene rings is involved in $\pi-\pi$ stacking interactions, and the two molecules are twisted considerably to allow intermolecular H-bonds to form. Thus, peptide **2a** or **2b** most likely exists as double helix **2B1** that gains its stability from both H-bonding and aromatic stacking interactions.

The behavior of **1** and **2** can be explained by the different intramolecular H-bonds involving the βAla or Gly residue and aromatic residue A or A′ (Figure 5, bottom). In **1**, the NH group of the βAla residue is part of an intramolecularly H-bonded six-membered ring that involves the phenolic oxygen of residue A; In **2**, the NH bond attached to residue A′ forms a intramolecularly H-bonded six-membered ring and another five-membered ring involving the carbonyl group of the Gly residue, which constitutes a three-center H-bond that is especially robust as demonstrated by our previous studies.[27] Such a three-center H-bond enforces coplanarity on residues A′ and Gly in **2**, as revealed by the structure **2B1** (Figure 5b), which allows **2** to only adopt an extended helical conformation. In contrast, no such three-center H-bond involving residues A and βAla of **1** exists, which offers sufficient flexibility for the βAla-Gly segment of **1** to serve as the loop of hairpin **1A**.

Validation of Hairpin and Double Helical Conformations. Conclusive evidence confirming the folded conformations of hybrid peptides **1** and **2** is provided by 2D ^{1}H NMR spectra. The NOESY spectrum of **1** recorded in $CDCl_3$ contains multiple NOEs that are fully consistent with hairpin **1A**. The most diagnostic NOEs include strong ones between protons *l* and *m*, and *f* and *f*1 (Figure 6), indicating that these

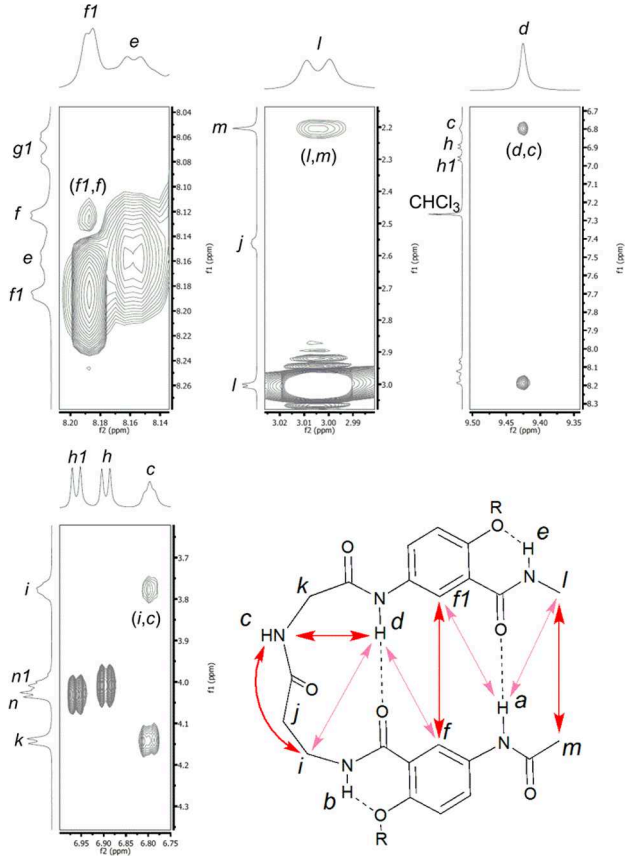

Figure 6. Partial NOESY spectra containing major NOEs revealed with **1** (5 mM, 500 MHz, 25 °C, mixing time: 500 ms) in $CDCl_3$. Major NOEs are indicated with arrows with the darker arrows indicating strong NOEs and the lighter ones indicating NOEs of medium strength.

protons are indeed placed into close proximity in the hairpin conformation of **1**. A very strong NOE between protons *c* and *i* was also observed, which, along with a strong NOE between *c* and *d*, demonstrates that the Gly and βAla residues constitute the loop of the expanded β-turn. In addition, NOEs between remote protons *a* and *f*1, *a* and *l*, *d* and *f*, and *d* and *i* further support the hairpin conformation adopted by **1**.

DOI: 10.1021/jacs.9b06094
J. Am. Chem. Soc. 2019, 141, 14239−14248

Three interproton distances determined based on NOEs (with the mixing time selected from a NOE buildup) between protons *a* and *f*1, *d* and *f*, and *m* and *l* of **1** and the same three distances based on energy-minimized conformation **1A** show good agreement, with errors of 1.2, 3.1 and 4.8% (Table S6). The computations were performed in gas phase at 0 K, and the NMR experiments were in $CDCl_3$. So solvent and finite temperature effects may be responsible for the differences. These results demonstrate that the computationally optimized hairpin does reflect the folded structure.

The expanded β-turn revealed with **1** represents a simple but extraordinary hairpin motif since the α/β dipeptide sequence, consisting of Gly and βAla, the conformationally most flexible α- and β-amino acid residues, results in a highly flexible loop. In fact, the expanded β-turn adopted by **1** is very unusual given that the formation of known natural or expanded β-turns requires the presence of at least one turn-promoting or conformationally constrained residue, such as aminoisobutyric acid (Aib) or Pro, in their dipeptide loops.[28]

The NOESY spectra of both **2a** and **2b**, recorded at −45 °C, at which all of the ^{1}H resonances are well dispersed, are very similar. As shown in Figure 7, the NOESY spectrum of **2b**

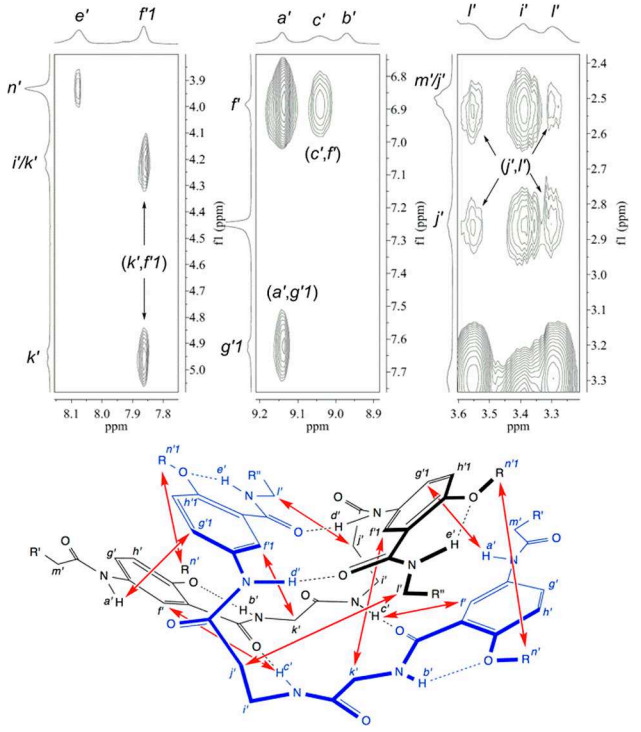

Figure 7. Partial NOESY spectra containing major NOEs revealed with **2b** (5 mM, 400 MHz, −45 °C, mixing time: 500 ms) in $CDCl_3$. Major NOEs are indicated with arrows.

contains strong NOEs between protons *a*′ and *g*′1, *c*′ and *f*′, *f*′1 and *k*′, and *j*′ and *l*′. Other NOEs include two with medium strength between *c*′ and *d*′, *d*′ and *l*′ (Figure S6). All strong and medium NOEs can be accounted for by the optimized conformation of dimer **2B1**. For example, the strong NOEs between protons *c*′ and *f*′, and *j*′ and *l*′ are consistent with the predicted pairing of the two H-bonding segments of **2B1**; those between protons *a*′ and *g*′1 are diagnostic of the stacked aromatic rings.

Comparing computed interproton distances of **2B1** with those derived from the NOEs (with the mixing time selected from a NOE buildup) of **2b** revealed that the computed distances are consistent with the NOE-derived distances, with errors between computed and measured values ranging from 2.8% to 9.6% (Table S7a). In contrast, the interproton distances based on structure **2B2** and the NOE-based distances show very large discrepancies, with errors ranging from 7.4% to 190.8% between computed and measured values (Table S7b). These results demonstrate that the optimized double helix **2B1** reflects the double-helical conformation of **2** in solution; i.e., tetrapeptides **2** exist as double helix **2B1**, not **2B2**.

Extended helix **2B** and its dimer **2B1** have few precedents among synthetic foldamers.[29,30] Gaining its stability from interstrand H-bonding and aromatic stacking interactions, such a double helical conformation is reminiscent of duplex DNAs but is based on a much simpler and easily modifiable structural scaffold.

Generalization of the Observed Folding/Assembling Behavior. The designs of **1** and **2** allow ready structural modification. For example, the Gly and βAla residues can be replaced with other chiral α- and β-amino acids. To probe the generality of the folding and assembling behavior observed with **1** and **2**, L-alanine and L-β-homoalanine was introduced to give oligomers **1a** and **1b**, or **2c** and **2d** (Figure 8).

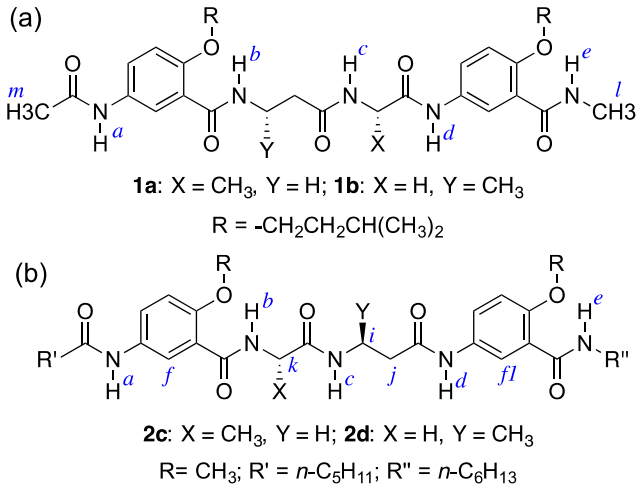

Figure 8. Structures of hybrid peptides (a) **1a** and **1b** derived from **1**, and (b) **2c** and **2d** derived from **2**.

Expanded β-Turns with Tunable Stability. The NOESY spectra of **1a** and **1b** reveal multiple strong NOEs between remote protons (Figures S7 and S8). These NOEs, similar to those that reveal the hairpin conformation of **1**, demonstrate that **1a** and **1b** fold into the same expanded β-turns.

The relative folding stability of **1**, **1a**, and **1b** were probed by comparing temperature-dependent shifts of the resonances of protons *a* and *d* that are intramolecularly H-bonded in the hairpin conformations. From 0 to 45 °C, the smallest upfield shifts, 0.24 and 0.18 ppm, respectively, were given by **1b**, followed by 0.33 and 0.22 ppm for **1**, and 0.33 and 0.27 ppm for **1a** (Table S8). These results show that replacing βAla of **1** with L-β-homoAla enhances the stability of the hairpin conformation of **1b**, while replacing the Gly residue with L-Ala gives **1a** with a hairpin conformation that is slightly less stable.

DOI: 10.1021/jacs.9b06094
J. Am. Chem. Soc. 2019, 141, 14239−14248

That the folded structure of **1b** is indeed more stable than that of **1** was shown by monitoring ROE contacts between terminal protons *l* and *m* that are brought into close proximity in the hairpin conformations. ROESY spectra recorded in $CDCl_3$ containing different proportions of CD_3OD at 0 °C indicate that for **1**, the end-to-end ROE contact between protons *l* and *m* could be detected with up to 55% CD_3OD (Figure S9), while for **1b**, the same ROE remained in the solvent with up to 95% CD_3OD (Figure S10). These results indicate that introducing a L-*β*-homoAla residue greatly enhances the stability of the resultant *β*-turn. It is expected that screening additional *β*-amino acid residues could uncover expanded *β*-turns with stability in highly competitive media, even water.

Double Helices with Biased Handedness and Enhanced Stability. The presence of chiral amino acid residue in **2c** or **2d** should result in two possible diastereomeric double helices with different stabilities, and thus bias the helical sense for the double helices of **2c** or **2d**. Consequently, the rapid helix inversion shown by **2a** or **2b** will be hampered for the helices of **2c** and **2d** (Figure 9).

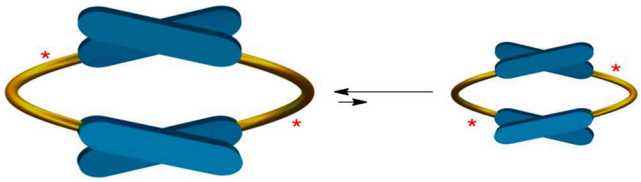

Figure 9. Schematic representation of the equilibrium of a pair of diastereomeric double helices resulting from introducing a chiral amino acid residue (*) into oligomer **2**.

Unlike the severely broadened resonances of methylene protons *i*, *j*, and *k* of the Gly and *β*Ala residues of **2a** and **2b** at 25 °C (Figures 2b and S1), well-dispersed ^{1}H NMR peaks are found for the corresponding methylene protons of **2c** and **2d** at this temperature (Figures S11), indicating hampered helix inversion. While protons *i*, *j*, or *k* of **2a** and **2b** give a broad, single peak (Figures 2b and S1), the protons of each corresponding methylene groups of **2c** (protons *i* and *j*) and **2d** (protons *j* and *k*) give two well-separated peaks, a phenomenon observed with **2a** and **2b** only at −45 °C. Thus, bond rotation involving the methylene carbons of **2c** and **2d** is limited even at 25 °C, suggesting that **2c** or **2d** exists mainly as the left- or right-handed helix and the double helices of **2c** and **2d** are more stable than those of **2a** and **2b**.

The relative stabilities of the double helices of **2b**, **2c**, and **2d** were probed by comparing the upfield shifts of the intermolecularly H-bonded amide protons *c* and *d* from 0 to 45 °C. Protons *c* and *d* of **2d** give the smallest shifts of 0.29 and 0.24 ppm, respectively, followed by 0.32 and 0.27 ppm for **2c**, and 0.36 and 0.28 ppm for **2b** (Table S9). These results suggest that the double helices of **2c** and **2d**, with their chiral amino acid residues, have higher stabilities than that of **2b**.

That **2c** and **2d** exist as double helices was confirmed by numerous strong ROEs in their 2D (ROESY) spectra measured at 0 °C (Figures S12 and S13). ROESY was used for **2c** and **2d** because it gave the best results at 0 °C while NOESY failed to reveal NOE cross peaks at this temperature. The detected ROEs can be fully assigned to double helical conformations similar to those of **2a** and **2b**, indicating that **2c** and **2d** exist as double helices in which the L-Ala and L-*β*-homoAla residues are well accommodated.

The helical sense of the dominant double helix adopted by **2c** or **2d** was determined. Computational modeling revealed that **2c** favors the right-handed double helix, which is unambiguously demonstrated by the large difference in the stabilities of the left- and right-handed helices, with the right-handed helix being 20 kcal/mol more stable than the left-handed one (Figure S14). In the energy-minimized right-handed helix of **2c**, the two methyl side chains point to the same direction and engage in van der Waals interaction that stabilizes the double helical structure (Figures 10a and S14b);

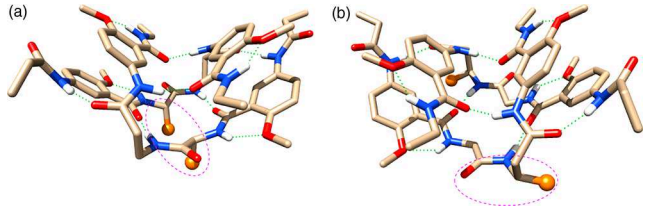

Figure 10. Energy-minimized structures of the dominant double helices of (a) **2c**, in which the two methyl side chains (orange balls) of the Ala residues (highlighted inside dashed purple circle) are arranged side-by-side and undergo van der Waals contact, and (b) **2d**, in which the methyl side chain (orange ball) of the *β*-homoAla residue and the C═O bond of the Ala residue (highlighted inside dashed purple circle) of the same molecule point away from each other.

while in the left-handed helix, the methyl side chains of the two L-Ala residues face each other in a head-on fashion (Figure S14a), causing disruption of intermolecular H-bonds and thus destabilizing the overall structure.

The only noticeable structural difference between the optimized double helices of **2d** is that, in the left-handed helix, the methyl side chain of each L-homoAla residue points away from the adjacent C═O bond of the Ala residues (Figures 10b and S15a), while in the right-handed helix, each methyl side chain is positioned next to the C═O bond, resulting in likely steric hindrance (Figure S15b). In fact, the left-handed helix is 3.7 kcal/mol more stable than the right-handed one. That **2d** exits as its left-handed double helix is experimentally confirmed by a strong ROE between the protons of L-homoAla methyl side chains and protons *f* on the N-terminal benzene residues (Figure S13). This ROE cannot be accounted for by the right-handed helix of **2d** in which the distance between the same methyl and protons *f* is about 5.5 Å (Figure S15a).

■ CONCLUSIONS

Differing only in their central *αβ* dipeptide sequences, hybrid tetrapeptides **1** and **2** exhibit distinct folding and assembling behavior. The turn formed by **1** is an unusual, expanded *β*-turn with a hybrid dipeptide sequence consisting of glycine and *β*-alanine that gives rise to a highly flexible *α*/*β* loop. In contrast to the 10-atom H-bonded ring typical of natural *β*-turns and their mimetics,[31] the turns of **1** contains a two-residue, 11-atom H-bonded ring. Tetrapeptides **2** fold into an extended helical conformation that further assembles into a quaternary structure. Such a feature is observed only with polypeptides and a few longer peptidomimetic oligomers.[32,33] The subtle structural difference between **1** and **2** results in completely different preorganization effected by intramolecular H-bonding

DOI: 10.1021/jacs.9b06094
J. Am. Chem. Soc. 2019, 141, 14239−14248

patterns that lead to the drastically different folding behavior of **1** and **2**. The generality of the folding and assembling behavior revealed with **1** and **2** is demonstrated by incorporating chiral α- and β-amino acids, L-alanine and L-β-homalanine, into **1** and **2**. The resultant derivatives **1a**, **1b**, **2c**, and **2d** follow the same folding and assembling patterns, forming expanded β-turns or extended helices that dimerize into double helices with enhanced stabilities at elevated temperature and in polar solvents, controlled chirality, and defined helical sense. The folding and assembly of these two groups of very short hybrid peptides have demonstrated the unique capability and versatility of synthetic foldamers in incorporating and combining natural and unnatural building blocks. The unexpected structural modules presented in this paper offer themselves as valuable scaffolds that allow the incorporation of a variety of α- and β-amino acid residues, a base on which interaction interfaces and functionalities in supramolecular biomimetic systems will be designed.

■ ASSOCIATED CONTENT

Supporting Information

The Supporting Information is available free of charge on the ACS Publications website at DOI: 10.1021/jacs.9b06094.

Synthetic procedures, experimental conditions, additional NMR spectra, mass spectra, and description of theoretical calculations (PDF)

■ AUTHOR INFORMATION

Corresponding Authors

*E-mail: bgong@buffalo.edu.

*E-mail: jinzhu@cioc.ac.cn.

ORCID

Daniel P. Miller: 0000-0003-1507-2667

Bo Song: 0000-0002-4337-848X

Erin S. Baker: 0000-0001-5246-2213

Huaqiang Zeng: 0000-0002-8246-2000

Xiaopeng Li: 0000-0001-9655-9551

Eva Zurek: 0000-0003-0738-867X

Bing Gong: 0000-0002-4155-9965

Author Contributions

⊗Y. Zhang and Y. Zhong contributed equally.

Notes

The authors declare no competing financial interest.

■ ACKNOWLEDGMENTS

This work was supported by the US Natural Science Foundation (CHE-1905094 to BG; MCB-1615570 to TS), the American Chemical Society − Petroleum Research Fund (PRF# 70641-ND, to BG), the Natural Science Foundation of China (NSFC 21072187 and 20772123, to JZ), the Silbert Fellowship from the University at Buffalo, SUNY (to DPM), and the Center of Computational Research, CCR, at the University at Buffalo (to EZ). We thank Jabin Gong for creating the art work.

■ REFERENCES

(1) (a) Gellman, S. H. Foldamers: a manifesto. *Acc. Chem. Res.* **1998**, *31*, 173. (b) Seebach, D.; Matthews, J. L. β-Peptides: a surprise at every turn. *Chem. Commun.* **1997**, 2015. (c) Hill, D. J.; Mio, M. J.; Prince, R. B.; Hughes, T. S.; Moore, J. S. A field guide to foldamers. *Chem. Rev.* **2001**, *101*, 3893. (d) Gong, B. Crescent oligoamides: from acyclic "macrocycles" to folding nanotubes. *Chem. - Eur. J.* **2001**, *7*, 4336. (e) Huc, I. Aromatic oligoamide foldamers. *Eur. J. Org. Chem.* **2004**, *2004*, 17. (f) Seebach, D.; Gardiner, J. β-Peptidic peptidomimetics. *Acc. Chem. Res.* **2008**, *41*, 1366. (g) Zhang, D.-W.; Zhao, X.; Hou, J.-L.; Li, Z.-T. Aromatic amide foldamers: structures, properties, and functions. *Chem. Rev.* **2012**, *112*, 5271. (h) Spencer, R.; Chen, K. H.; Manuel, G.; Nowick, J. S. Recipe for β-sheets: Foldamers containing amyloidogenic peptide sequences. *Eur. J. Org. Chem.* **2013**, *2013*, 3523. (i) Hartley, C. S. Folding of ortho-phenylenes. *Acc. Chem. Res.* **2016**, *49*, 646.

(2) Appella, D. H.; Christianson, L. A.; Karle, I. L.; Powell, D. R.; Gellman, S. H. β-Peptide foldamers: robust helix formation in a new family of β-amino acid oligomers. *J. Am. Chem. Soc.* **1996**, *118*, 13071.

(3) Seebach, D.; Overhand, M.; Kühnle, F. N. M.; Martinoni, B.; Oberer, L.; Hommel, U.; Widmer, H. β-Peptides. Synthesis by Arndt-Eistert homologation with concomitant peptide coupling. Structure determination by NMR and CD spectroscopy and by x-ray crystallography. Helical secondary structure of a β-hexapeptide in solution and its stability towards pepsin. *Helv. Chim. Acta* **1996**, *79*, 913.

(4) Hanessian, S.; Luo, X. H.; Schaum, R.; Michnick, S. Design of secondary structures in unnatural peptides: stable helical γ-tetra-, hexa-, and octapeptides and consequences of α-substitution. *J. Am. Chem. Soc.* **1998**, *120*, 8569.

(5) Szabo, L.; Smith, B. L.; McReynolds, K. D.; Parrill, A. L.; Morris, E. R.; Gervay, J. Solid phase synthesis and secondary structural studies of (1→5) amide-linked sialooligomers. *J. Org. Chem.* **1998**, *63*, 1074.

(6) Semetey, V.; Rognan, D.; Hemmerlin, C.; Graff, R.; Briand, J. P.; Marraud, M.; Guichard, G. Stable helical secondary structure in short-chain *N*, *N*′-linked oligoureas bearing proteinogenic side chains. *Angew. Chem., Int. Ed.* **2002**, *41*, 1893.

(7) (a) Wu, C. W.; Sanborn, T. J.; Huang, K.; Zuckermann, R. N.; Barron, A. E. Peptoid oligomers with α-chiral, aromatic side chains: sequence requirements for the formation of stable peptoid helices. *J. Am. Chem. Soc.* **2001**, *123*, 6778. (b) Butterfoss, G. L.; Yoo, B.; Jaworski, J. N.; Chorny, I.; Dill, K. A.; Zuckermann, R.; Bonneau, R.; Kirshenbaum, K.; Voelz, V. A. De novo structure prediction and experimental characterization of folded peptoid oligomers. *Proc. Natl. Acad. Sci. U. S. A.* **2012**, *109*, 14320.

(8) (a) Nelson, J. C.; Saven, J. G.; Moore, J. S.; Wolynes, P. G. Solvophobically driven folding of nonbiological oligomers. *Science* **1997**, *277*, 1793. (b) Jones, T. V.; Blatchly, R. A.; Tew, G. N. Synthesis of Alkoxy-Substituted ortho-Phenylene Ethynylene Oligomers. *Org. Lett.* **2003**, *5*, 3297.

(9) (a) Hamuro, Y.; Geib, S. J.; Hamilton, A. D. Novel folding patterns in a family of oligoanthranilamides: non-peptide oligomers that form extended helical secondary structures. *J. Am. Chem. Soc.* **1997**, *119*, 10587. (b) Zhu, J.; Parra, R. D.; Zeng, H. Q.; Skrzypczak-Jankun, E.; Zeng, X. C.; Gong, B. A New Class of Folding Oligomers: Crescent Oligoamides. *J. Am. Chem. Soc.* **2000**, *122*, 4219. (c) Jiang, H.; Léger, J. M.; Huc, I. Aromatic δ-Peptides. *J. Am. Chem. Soc.* **2003**, *125*, 3448. (d) Yan, Y.; Qin, B.; Shu, Y. L.; Chen, X. Y.; Yip, Y. K.; Zhang, D. W.; Su, H. B.; Zeng, H. Q. Helical Organization in foldable aromatic oligoamides by a continuous hydrogen-bonding network. *Org. Lett.* **2009**, *11*, 1201. (e) Singleton, M. L.; Pirotte, G.; Kauffmann, B.; Ferrand, Y.; Huc, I. Increasing the size of an aromatic helical foldamer cavity by strand intercalation. *Angew. Chem., Int. Ed.* **2014**, *53*, 13140. (f) Burslem, G. M.; Kyle, H. F.; Prabhakaran, P.; Breeze, A. L.; Edwards, T. A.; Nelson, A. S.; Warriner, S. L.; Wilson, A. J. Synthesis of highly functionalized oligobenzamide proteomimetic foldamers by late stage introduction of sensitive groups. *Org. Biomol. Chem.* **2016**, *14*, 3782. (g) Meisel, J. W.; Hu, C. H. T.; Hamilton, A. D. Mimicry of a β-hairpin turn by a nonpeptidic laterally flexible foldamer. *Org. Lett.* **2018**, *20*, 3879. (h) Urushibara, K.; Ferrand, Y.; Liu, Z. W.; Masu, H.; Pophristic, V.; Tanatani, A.; Huc, I. Frustrated helicity: Joining the diverging ends of a stable aromatic amide helix to form a fluxional macrocycle. *Angew. Chem., Int. Ed.* **2018**, *57*, 7888. (i) Liu, C. Z.; Koppireddi, S.; Wang, H.; Zhang, D. W.; Li, Z. T. Halogen Bonding Directed Supramolecular Quadruple and Double

Helices from Hydrogen-Bonded Arylamide Foldamers. *Angew. Chem., Int. Ed.* **2019**, *58*, 226.
(10) Hou, J. L.; Shao, X. B.; Chen, G. J.; Zhou, Y. X.; Jiang, X. K.; Li, Z. T. Hydrogen bonded oligohydrazide foldamers and their recognition for saccharides. *J. Am. Chem. Soc.* **2004**, *126*, 12386.
(11) (a) van Gorp, J. J.; Vekemans, J. A. J. M.; Meijer, E. W. Facile synthesis of a chiral polymeric helix; folding by intramolecular hydrogen bonding. *Chem. Commun.* **2004**, *1*, 60. (b) Zhang, A. M.; Han, Y. H.; Yamato, K.; Zeng, X. C.; Gong, B. Aromatic Oligoureas: Enforced Folding and Assisted Cyclization. *Org. Lett.* **2006**, *8*, 803. (c) Hu, T.; Connor, A. L.; Miller, D. P.; Wang, X.; Pei, Q.; Liu, R.; He, L.; Zheng, C.; Zurek, E.; Lu, Z. L.; Gong, B. Helical Folding of *meta*-Connected Aromatic Oligoureas. *Org. Lett.* **2017**, *19*, 2666.
(12) (a) Hua, Y.; Flood, A. H. Flipping the switch on chloride concentrations with a light-active foldamer. *J. Am. Chem. Soc.* **2010**, *132*, 12838. (b) Mathew, S.; Crandall, L. A.; Ziegler, C. J.; Hartley, C. S. Enhanced helical folding of ortho-phenylenes through the control of aromatic stacking interactions. *J. Am. Chem. Soc.* **2014**, *136*, 16666. (c) Shang, J.; Gallagher, N. M.; Bie, F. S.; Li, Q. L.; Che, Y. K. Y.; Jiang, H. aromatic triazole foldamers induced by C−H···X (X = F, Cl) intramolecular hydrogen bonding. *J. Org. Chem.* **2014**, *79*, 5134. (d) Jeon, H. G.; Jung, J. Y.; Kang, P. J.; Choi, M. G.; Jeong, K. S. Folding-generated molecular tubes containing one-dimensional water chains. *J. Am. Chem. Soc.* **2016**, *138*, 92. (e) Lister, F. G. A.; Eccles, N.; Pike, S. J.; Brown, R. A.; Whitehead, G. F. S.; Raftery, J.; Webb, S. J.; Clayden, J. Bis-pyrene probes of foldamer conformation in solution and in phospholipid bilayers. *Chem. Sci.* **2018**, *9*, 6860.
(13) Chung, Y. J.; Christianson, L. A.; Stanger, H. E.; Powell, D. R.; Gellman, S. H. A β-peptide reverse turn that promotes hairpin formation. *J. Am. Chem. Soc.* **1998**, *120*, 10555.
(14) Seebach, D.; Abele, S.; Gademann, K.; Jaun, B. Pleated sheets and turns of β-peptides with proteinogenic side chains. *Angew. Chem., Int. Ed.* **1999**, *38*, 1595.
(15) Sebaoun, L.; Maurizot, V.; Granier, T.; Kauffmann, B.; Huc, I. Aromatic oligoamide β-sheet foldamers. *J. Am. Chem. Soc.* **2014**, *136*, 2168.
(16) (a) Lokey, R. S.; Iverson, B. L. Synthetic molecules that fold into a pleated secondary structure in solution. *Nature* **1995**, *375*, 303. (b) Bisson, A. P.; Carver, F. J.; Eggleston, D. S.; Haltiwanger, R. C.; Hunter, C. A.; Livingstone, D. L.; McCabe, J. F.; Rotger, C.; Rowan, A. E. Synthesis and recognition properties of aromatic amide oligomers: Molecular zippers. *J. Am. Chem. Soc.* **2000**, *122*, 8856. (c) ten Cate, A. T.; Kooijman, H.; Spek, A. L.; Sijbesma, R. P.; Meijer, E. W. Conformational control in the cyclization of hydrogen-bonded supramolecular polymers. *J. Am. Chem. Soc.* **2004**, *126*, 3801. (d) ten Cate, A. T.; Dankers, P. Y. W.; Sijbesma, R. P.; Meijer, E. W. Disulfide exchange in hydrogen-bonded cyclic assemblies: Stereochemical self-selection by double dynamic chemistry. *J. Org. Chem.* **2005**, *70*, 5799. (e) Delsuc, N.; Godde, F.; Kauffmann, B.; Léger, J.-M.; Huc, I. The Herringbone Helix A Noncanonical Folding in Aromatic Aliphatic Peptides. *J. Am. Chem. Soc.* **2007**, *129*, 11348. (f) Gooch, A.; Barrett, S.; Fisher, J.; Lindsay, C. I.; Wilson, A. J. Ditopic triply hydrogen-bonded heterodimers. *Org. Biomol. Chem.* **2011**, *9*, 5938. (g) Nair, R. V.; Kheria, S.; Rayavarapu, S.; Kotmale, A. S.; Jagadeesh, B.; Gonnade, R. G.; Puranik, V. G.; Rajamohanan, P. R.; Sanjayan, G. J. A Synthetic Zipper Peptide Motif Orchestrated via Co-operative Interplay of Hydrogen Bonding, Aromatic Stacking, and Backbone Chirality. *J. Am. Chem. Soc.* **2013**, *135*, 11477. (h) Priya, G.; Kotmale, A. S.; Chakravarty, D.; Puranik, V. G.; Rajamohanan, P. R.; Sanjayan, G. J. Conformational modulation of peptides using β-amino benzenesulfonic acid (SAnt). *Org. Biomol. Chem.* **2015**, *13*, 2087.
(17) (a) Horne, W. S.; Gellman, S. H. Foldamers with heterogeneous backbones. *Acc. Chem. Res.* **2008**, *41*, 1399. (b) Nowick, J. S.; Chung, D. M.; Maitra, K.; Maitra, S.; Stigers, K. D.; Sun, Y. An unnatural amino acid that mimics a tripeptide β-strand and forms β-sheetlike hydrogen-bonded dimers. *J. Am. Chem. Soc.* **2000**, *122*, 7654. (c) Hayen, A.; Schmitt, M. A.; Ngassa, F. N.; Thomasson, K. A.; Gellman, S. H. Two helical conformations from a single foldamer backbone: "split personality" in short alpha/beta-peptides. *Angew. Chem., Int. Ed.* **2004**, *43*, 505. (d) Patgiri, A.; Joy, S. T.; Arora, P. S. Nucleation effects in peptide foldamers. *J. Am. Chem. Soc.* **2012**, *134*, 11495.
(18) (a) Gong, B. Engineering hydrogen-bonded duplexes. *Polym. Int.* **2007**, *56*, 436. (b) Gong, B.; Yan, Y.; Zeng, H.; Skrzypczak-Jankunn, E.; Kim, Y. W.; Zhu, J.; Ickes, H. A new approach for the design of supramolecular recognition units: hydrogen-bonded molecular duplexes. *J. Am. Chem. Soc.* **1999**, *121*, 5607.
(19) (a) Zeng, H. Q.; Yang, X. W.; Flowers, R. A.; Gong, B. A Noncovalent Approach to Antiparallel β-Sheet Formation. *J. Am. Chem. Soc.* **2002**, *124*, 2903. (b) Shi, Y. D.; Tang, Q.; Jiang, Y. F.; Pei, Q.; Tan, H. W.; Lu, Z. L.; Gong, B. Effective formation of stable and versatile double-stranded β-sheets templated by a hydrogen-bonded duplex. *Chem. Commun.* **2018**, *54*, 3719.
(20) Yang, X. W.; Hua, F. J.; Yamato, K.; Ruckenstein, E.; Gong, B.; Kim, W.; Ryu, C. Y. Supramolecular AB Diblock Copolymers. *Angew. Chem., Int. Ed.* **2004**, *43*, 6471.
(21) Yang, X. W.; Gong, B. Template-Assisted Cross Olefin Metathesis. *Angew. Chem., Int. Ed.* **2005**, *44*, 1352.
(22) (a) Mei, J.; Graham, K. R.; Stalder, R.; Reynolds, J. R. Synthesis of isoindigo-based oligothiophenes for molecular bulk heterojunction solar cells. *Org. Lett.* **2010**, *12*, 660. (b) Lee, O. P.; Yiu, A. T.; Beaujuge, P. M.; Woo, C. H.; Holcombe, T. W.; Millstone, J. E.; Douglas, J. D.; Chen, M. S.; Fréchet, J. M. Efficient small molecule bulk heterojunction solar cells with high fill factors via pyrene-directed molecular self-assembly. *Adv. Mater.* **2011**, *23*, 5359. (c) Loser, S.; Bruns, C. J.; Miyauchi, H.; Ortiz, R. P.; Facchetti, A.; Stupp, S. I.; Marks, T. J. A Naphthodithiophene-Diketopyrrolopyrrole Donor Molecule for Efficient Solution-Processed Solar Cells. *J. Am. Chem. Soc.* **2011**, *133*, 8142. (d) Welch, G. C.; Perez, L. A.; Hoven, C. V.; Zhang, Y.; Dang, X.-D.; Sharenko, A.; Toney, M. F.; Kramer, E. J.; Nguyen, T.-Q.; Bazan, G. C. A modular molecular framework for utility in small-molecule solution-processed organic photovoltaic devices. *J. Mater. Chem.* **2011**, *21*, 12700. (e) Holcombe, T. W.; Yum, J.-H.; Yoon, J.; Gao, P.; Marszalek, M.; Di Censo, D.; Rakstys, K.; Nazeeruddin, M. K.; Graetzel, M. A structural study of DPP-based sensitizers for DSC applications. *Chem. Commun.* **2012**, *48*, 10724. (f) Sun, Y.; Welch, G. C.; Leong, W. L.; Takacs, C. J.; Bazan, G. C.; Heeger, A. J. M. Solution-processed small-molecule solar cells with 6.7% efficiency. *Nat. Mater.* **2012**, *11*, 44. (g) Zerdan, R. B.; Shewmon, N. T.; Zhu, Y.; Mudrick, J. P.; Chesney, K. J.; Xue, J. G.; Castellano, R. K. The influence of solubilizing chain stereochemistry on small molecule photovoltaics. *Adv. Funct. Mater.* **2014**, *24*, 5993.
(23) (a) Etter, M. C. Encoding and decoding hydrogen-bond patterns of organic compounds. *Acc. Chem. Res.* **1990**, *23*, 120−126. (b) Bernstein, J.; Davis, R. E.; Shimoni, L.; Chang, N.-L. Patterns in hydrogen bonding: Functionality and graph set analysis in crystals. *Angew. Chem., Int. Ed. Engl.* **1995**, *34*, 1555. (c) Holmes, D. L.; Smith, E. M.; Nowick, J. S. Solid-phase synthesis of artificial β-sheets. *J. Am. Chem. Soc.* **1997**, *119*, 7665.
(24) Bain, A. D. Chemical exchange in NMR. *Prog. Nucl. Magn. Reson. Spectrosc.* **2003**, *43*, 63.
(25) Grimme, S.; Antony, J.; Ehrlich, S.; Krieg, H. A consistent and accurate *ab initio* parametrization of density functional dispersion correction (DFT-D) for the 94 elements H-Pu. *J. Chem. Phys.* **2010**, *132*, 154104.
(26) te Velde, G.; Bickelhaupt, F. M.; Baerends, E. J.; Fonseca Guerra, C.; van Gisbergen, S. J. A.; Snijders, J. G.; Ziegler, T. Chemistry with ADF. *J. Comput. Chem.* **2001**, *22*, 931.
(27) Parra, R. D.; Zeng, H. Q.; Zhu, J.; Zheng, C.; Zeng, X. C.; Gong, B. Stable Three-center hydrogen bonding in a partially rigidified structure. *Chem. - Eur. J.* **2001**, *7*, 4352.
(28) Chatterjee, S.; Roy, R. S.; Balaram, P. Expanding the polypeptide backbone: hydrogen-bonded conformations in hybrid polypeptides containing the higher homologues of alpha-amino acids. *J. R. Soc., Interface* **2007**, *4*, 587.
(29) Berl, V.; Khoury, R. G.; Huc, I.; Krische, M. J.; Lehn, J. M. Interconversion of single and double helices formed from synthetic molecular strands. *Nature* **2000**, *407*, 720.

DOI: 10.1021/jacs.9b06094
J. Am. Chem. Soc. 2019, 141, 14239−14248

(30) Stross, A. E.; Iadevaia, G.; Nunez-Villanueva, D.; Hunter, C. A. Sequence-selective formation of synthetic H-bonded duplexes. *J. Am. Chem. Soc.* **2017**, *139*, 12655.
(31) (a) Liang, G. B.; Rito, C. J.; Gellman, S. H. Thermodynamic Analysis of β-Turn Formation in Pro-Ala, Pro-Gly, and Pro-Val Model Peptides in Methylene Chloride. *J. Am. Chem. Soc.* **1992**, *114*, 4440. (b) Haque, T. S.; Little, J. C.; Gellman, S. H. Stereochemical Requirements for β-Hairpin Formation: Model Studies with Four-Residue Peptides and Depsipeptides. *J. Am. Chem. Soc.* **1996**, *118*, 6975. (c) Nowick, J. S.; Lam, K. S.; Khasanova, T. V.; Kemnitzer, W. E.; Maitra, S.; Mee, H. T.; Liu, R. W. An unnatural amino acid that induces β-sheet folding and interaction in peptides. *J. Am. Chem. Soc.* **2002**, *124*, 4972.
(32) Collie, G. W.; Bailly, R.; Pulka-Ziach, K.; Lombardo, C. M.; Mauran, L.; Taib-Maamar, N.; Dessolin, J.; Mackereth, C. D.; Guichard, G. Molecular recognition within the cavity of a foldamer helix bundle: encapsulation of primary alcohols in aqueous conditions. *J. Am. Chem. Soc.* **2017**, *139*, 6128.
(33) George, K. L.; Horne, W. S. Foldamer tertiary structure through sequence-guided protein backbone alteration. *Acc. Chem. Res.* **2018**, *51*, 1220.

DOI: 10.1021/jacs.9b06094
J. Am. Chem. Soc. 2019, 141, 14239−14248